Iron-based Heusler compounds Fe_2YZ: Comparison with theoretical predictions of the crystal structure and magnetic properties

T. Gasi,[1] V. Ksenofontov,[1] J. Kiss,[2] S. Chadov,[2] A. K. Nayak,[2] M. Nicklas,[2] J. Winterlik,[1] M. Schwall,[1] P. Klaer,[3] P. Adler,[2,*] and C. Felser[1,2,†]

[1]*Institut für Anorganische und Analytische Chemie, Johannes Gutenberg-Universität, 55128 Mainz, Germany*

[2]*Max-Planck-Institut für Chemische Physik fester Stoffe, 01187 Dresden, Germany*

[3]*Institut für Physik, Johannes Gutenberg-Universität, 55099 Mainz, Germany*

(Received 5 December 2012; published 8 February 2013)

The present work reports on the new soft ferromagnetic Heusler phases Fe_2NiGe, Fe_2CuGa, and Fe_2CuAl, which in previous theoretical studies have been predicted to exist in a tetragonal Heusler structure. Together with the known phases Fe_2CoGe and Fe_2NiGa these materials have been synthesized and characterized by powder x-ray diffraction, ^{57}Fe Mössbauer spectroscopy, superconducting quantum interference device, and energy-dispersive x-ray measurements. In particular Mössbauer spectroscopy was used to monitor the degree of local atomic order/disorder and to estimate magnetic moments at the Fe sites from the hyperfine fields. It is shown that in contrast to the previous predictions all the materials except Fe_2NiGa basically adopt the inverse cubic Heusler (X) structure with differing degrees of disorder. The experimental data are compared with results from *ab initio* electronic structure calculations on local-density approximation level incorporating the effects of atomic disorder by using the coherent potential approximation. A good agreement between calculated and experimental magnetic moments is found for the cubic inverse Heusler phases. Model calculations on various atomic configurations demonstrate that antisite disorder tends to enhance the stability of the X structure.

DOI: 10.1103/PhysRevB.87.064411 PACS number(s): 75.50.Cc, 71.20.Gj, 75.30.Cr, 76.80.+y

I. INTRODUCTION

Magnetic Heusler compounds with the general formula X_2YZ where X and Y are transition-metal elements and Z is a main group element are one of the most fascinating classes of modern magnetic materials, from both a fundamental as well as an application-oriented point of view.[1,2] The large variety of physical properties which can be realized in Heusler-type materials is a consequence of their peculiar crystal structure and their great chemical flexibility. The basic cubic $L2_1$ crystal structure of X_2YZ phases (space group $Fm\bar{3}m$) is composed of four interpenetrating fcc sublattices (see Fig. 1). It may be considered as a zinc-blende-like arrangement of Z and X atoms with the remaining X atoms in the tetrahedral and the Y atoms in the octahedral voids. This leads to a NaCl-type arrangement of the Y and Z atoms where each Y atom is surrounded by six Z atoms in the second coordination sphere, whereas the nearest neighbors of each Y atom are eight X atoms. On the other hand, each X atom is surrounded by four Y and four Z atoms. An early contribution to the rationalization of the magnetic properties of Heusler compounds is the theoretical work by Kübler *et al.* on X_2MnZ-type compounds,[3] which describes how large localized magnetic moments in the Mn sublattice are realized by an itinerant electronic system composed of hybridized Mn $d-X$ d bands.[3] Kübler *et al.* emphasized the importance of indirect Mn-Z-Mn interactions for the magnetic properties. The various magnetoresponsive effects of Heusler compounds such as magnetic-field-induced shape memory/strain effects, magnetoresistance, and magnetocaloric effects[4,5] promise a wide range of applications. For instance, ferromagnetic martensites are experimentally found in different half Heusler alloys such as NiMnGa, NiFeGa, CoNiGa, and related materials.[6] All these effects occur in temperature ranges which are convenient for device operation. The great current interest in Heusler compounds arises, however, at least partly from the observation of half metallic ferromagnetism in several of these materials[1,7] as half metallic ferromagnets have a great potential in the emerging field of spintronic applications.[8,9] Since Wurmehl *et al.* have reported an exceptionally high magnetic moment of $6\mu_B$ and a Curie temperature T_C of 1100 K for the half metallic Co_2FeSi,[10] the interest for Heusler compounds has highly increased, and the Co-based Heusler compounds have been studied extensively.[2] The combination of Co and Fe is particularly good for obtaining high T_C's.

Not only the cubic but also tetragonally distorted Heusler compounds, like Mn_3Ga,[11] have found considerable attention as they are attractive candidates for spin-transfer-torque applications.[12] In this respect it is remarkable that in the course of a recent theoretical study on potentially new Heusler compounds[13,14] several iron-based Fe_2YZ materials with a regular tetragonal Heusler structure have been predicted.[14] Actually it was found for these phases that the inverse cubic Heusler structure (X structure, space group $F\bar{4}3m$), should be more stable than the regular one (see Fig. 1). The X structure may be formally written as (FeY)FeZ where the Fe atoms occupy the octahedral and tetrahedral voids of the zinc-blende-type lattice to equal parts. These two Fe sites will be denoted as Fe(A) and Fe(B), respectively. The inverse Fe_2YZ structures in some of the materials are, however, predicted to be unstable towards a tetragonal distortion which tends to maximize the bonding interactions.[14] Motivated by the potential importance of tetragonal iron-based Heusler compounds for applications, especially as potential rare-earth free hard magnets, and by the fundamental question of electronic instabilities in Heusler compounds, this work reports the synthesis and characterization of the new compounds Fe_2NiGe, Fe_2CuGa, and Fe_2CuAl, the existence of which

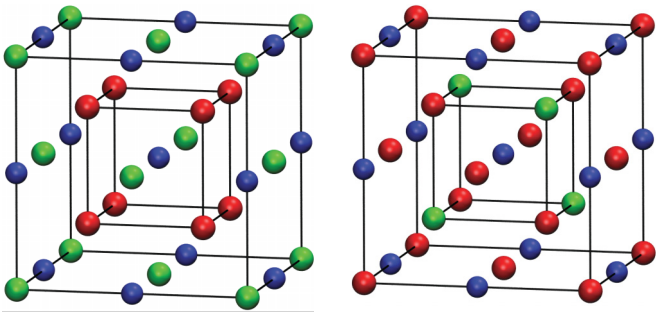

(a) (b)

FIG. 1. (Color online) Conventional unit cell of the cubic Heusler (a) and inverse Heusler (b) X_2YZ compounds. The X, Y, and Z atom types, where X = Fe for the materials studied in this paper, are shown with red, green, and blue spheres, respectively. In (b) the Fe atoms adopt two distinct sites denoted as Fe(A) and Fe(B) in the text. Fe(A) is located in octahedral voids (outer cube), Fe(B) in the tetrahedral voids (inner cube) of the zinc-blende-type lattice.

has been predicted in Ref. 14. In addition, the properties of the known phases Fe_2CoGe (Ref. 15) and Fe_2NiGa (Ref. 16) have been investigated in more detail. Usually first-principles electronic structure calculations are based on a perfect crystal. However, Heusler compounds are ternary or even quaternary compounds which are widely amenable to chemical disorder. This can be the reason for discrepancies between theoretical predictions and experimental results. This aspect turns out to be of crucial importance also for the present Fe_2YZ materials and therefore will be discussed in detail. As x-ray diffraction (XRD) techniques are frequently insufficient for extracting the detailed atomic order in Heusler materials additional experimental methods are required. Anomalous XRD and extended x-ray-absorption fine-structure (EXAFS) experiments are versatile techniques for this purpose,[17] while x-ray magnetic circular dichroism (XMCD) studies give access to site-selective magnetic moments.[18,19] In the case of the present iron-based materials we have used ^{57}Fe-Mössbauer spectroscopy as a simple laboratory technique to characterize both the local atomic and magnetic order in our samples. The additional theoretical analysis based on first-principles electronic structure calculations treating the chemical disorder by means of the CPA method[20,21](coherent potential approximation) shows that the cubic structure of Fe_2YZ Heusler materials becomes indeed more stable when assuming a certain degree of antisite disorder as suggested by the experiments.

II. SYNTHESIS AND CHARACTERIZATION

A. Experimental details

Fe_2YZ (Y = Co, Ni, Cu; Z = Al, Ga, Ge) compounds were synthesized by repeated arc melting or ball milling of stoichiometric amounts of pure metals in an argon atmosphere under 10^{-4} mbar pressure. To ensure an oxygen-free atmosphere, titanium was used as getter material. The samples were three times melted and turned over. The weight loss after the whole process was less than 0.5%. Additionally, they were annealed in evacuated glass quartz tubes for two weeks at 673 K and then in order to test the influence of the annealing temperature on the degree of disorder some of them were further annealed at 1173 K. After annealing they were quenched in a mixture of ice and water. In addition it has been attempted to synthesize Fe_2ZnAl in a similar way, however, the Heusler phase could not be stabilized. The crystal structures of the products at room temperature were investigated by means of powder XRD using excitation by monochromatic Cu-$K_{\alpha 1}$ ($\lambda_{\mathrm{Cu},K\alpha 1} = 1.540\,598$ Å) or Mo-$K_{\alpha 1,2}$ radiation ($\lambda_{\mathrm{Mo},K\alpha 1} = 0.709\,316\,5$ Å) in θ-θ scanning mode. Disc-shaped samples were used for Fe_2CoGe, Fe_2NiGa, Fe_2CuGa, and Fe_2CuAl. Since Fe_2NiGe samples were better produced by ball milling, they were measured as powders. The XRD patterns were fitted by the FULLPROF software package;[22] in the case of Mo-$K_{\alpha 1,2}$ radiation the α_1/α_2 splitting of the radiation was taken into account. The magnetization was measured by different superconducting quantum interference device (SQUID) magnetometers (MPMS-XL5 and MPMS SQUID VSM, Quantum Design) within the temperature range 1.8–950 K. ^{57}Fe-Mössbauer measurements were performed in transmission, backscattering, and CEMS (conversion electron Mössbauer spectroscopy) modes using a constant acceleration spectrometer with a ^{57}Co (Rh matrix) source with $h\nu$ = 14.4 keV. The backscattering spectra were recorded with the miniaturized Mössbauer spectrometer MIMOS.[23] Information about bulk properties was obtained from the transmission or backscattering spectra (information depth $d \sim 10\mu$m), while the CEM spectra ($d \sim 100$ nm) are more surface sensitive. To obtain the reliable distribution of hyperfine parameters the data were fitted using the Voigt-based fitting (VBF) model within the RECOIL software package.[24]

The homogeneity and stoichiometry of the samples was controlled by a scanning electron microscope (SEM, Jeol JSM-6400) equipped with an energy-dispersive x-ray (EDX) spectroscopy detection system (EUMEX EDX). The measurements were carried out at 3×10^{-6} mbar pressure. The acceleration voltage of 20 kV with inspection angle of 35° was used. For the correction of the quantitative data the so-called ZAF method was applied, which relies on atomic number (Z), and on absorption (A) and fluorescence (F) effects. The images were acquired via the Digital Image Processing System (DIPS) and the quantitative chemical analysis was performed with the WINEDS 4.0 program. According to the EDX analysis the Fe_2YZ alloys show a rather good homogeneity in their composition, except Fe_2NiGe (see Table I).

B. XRD structural characterization

Typically well-ordered Heusler compounds crystallize in a cubic crystal structure, either in the regular $L2_1$ (space group

TABLE I. Relative concentration given as percentages of the samples from the Fe_2YZ alloys according to an EDX analysis.

Compound	Fe	Y	Z
Fe_2CoGe	50.43	25.36	24.22
Fe_2CuGa	49.77	25.94	24.30
Fe_2NiGa	50.78	24.65	24.57
Fe_2NiGe	47.48	27.55	24.97
Fe_2CuAl	48.32	26.57	25.11

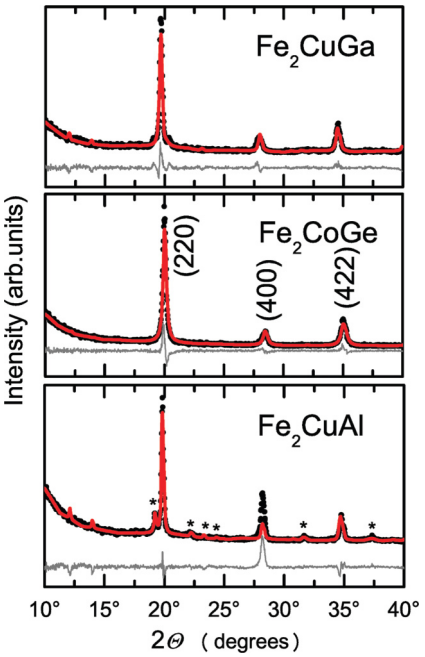

FIG. 2. (Color online) XRD of Fe_2CuGa, Fe_2CoGe, and Fe_2CuAl alloys annealed at 673 K. The diffraction patterns are compared to the results of Rietveld refinements. Diffraction peaks marked with stars are assigned to an impurity phase Cu_xAl_y (Ref. 25) (space group $Fm\bar{3}m$ with $a = 3.63$ Å). The measurements were carried out at RT using Mo-K_α radiation.

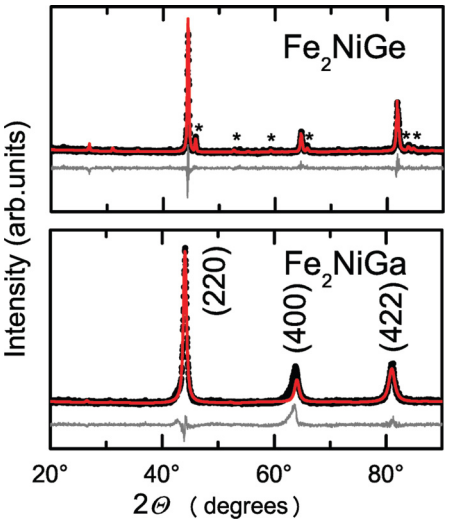

FIG. 3. (Color online) XRD of Fe_2NiGe and Fe_2NiGa alloys annealed at 673 K. The diffraction patterns are compared to the results of Rietveld refinements. Diffraction peaks marked with stars are assigned to an impurity phase Fe_xGe (Ref. 26) (space group $P6_3/mmc$ with $a = 3.97$ Å and $c = 5.05$ Å). The measurements were carried out at RT using Cu-K_α radiation.

$Fm\bar{3}m$) or in the inverse X (space group $F\bar{4}3m$) structure. For both structure types the XRD patterns exhibit additional (111) and (200) fcc superstructure reflections. In many cases the intensity ratio I_{111}/I_{200} allows us to distinguish them from each other. Based on plane-wave pseudopotential calculations, some of the present materials have been predicted to crystallize in a tetragonally distorted regular Heusler structure (space group $P4_2/ncm$).[14] The XRD patterns of the Fe_2YZ materials annealed at 673 K are shown in Figs. 2 and 3. As is seen from the typical distances between the (220), (400), and (422) reflections (note that the Miller indices correspond to an fcc lattice) all materials crystallize in a cubic structure. Additional weak reflections in the patterns of Fe_2NiGe, Fe_2CuGa, and Fe_2CuAl point to the presence of a small fraction of impurity phases. However, none of the patterns indicate any features like peak splittings which could be attributed to a tetragonal distortion predicted for Fe_2NiGe, Fe_2CuGa, and Fe_2CuAl.[14] The lattice parameters obtained from Rietveld refinement of the data by assuming the inverse cubic Heusler structure (space group $F\bar{4}3m$) are given in Table II. The fcc superstructure reflections are not discernible in any of the XRD patterns. Two reasons have to be considered for that. First, the samples may be disordered according to the $A2$ type (with all lattice sites randomly occupied by the constituting elements). This results in a bcc-type ($Pm\bar{3}m$) diffraction pattern, where no superstructure reflections appear. Second, in all compounds except Fe_2CuAl the constituting elements are entirely from the fourth row of the Periodic Table, which results in similar scattering factors. This leads to a virtual extinction of the (111) and (200) reflections, or at least, to very low intensities, if the standard laboratory sources with Cu-K_α or Mo-K_α radiation are used. In fact for a well-ordered sample of Fe_2CoGe very weak superstructure reflections have been observed.[15] Their detection requires, however, an improved signal-to-noise ratio of the XRD patterns and thus considerably longer measurement times. For studying the influence of the annealing temperature on the sample quality, in addition to the samples annealed at 673 K, the XRD patterns of samples annealed at 1173 K have been also recorded. In the case of Fe_2NiGa and Fe_2CuAl sample decomposition was observed (XRD patterns not shown); the XRD patterns of the other samples (Fig. 4) revealed only minor changes. The phase purity of Fe_2NiGe appears to be slightly improved by annealing at higher temperature, but the Mössbauer spectra still revealed an impurity signal. Therefore, if not explicitly stated otherwise, we will focus in the rest of the paper on the samples annealed at 673 K.

In summary, the XRD patterns verify that the synthesized Fe_2YZ materials all crystallize in cubic Heusler-type structures. It is, however, impossible to derive the exact atomic order from the XRD data. More information about the atomic and magnetic order is obtained by ^{57}Fe-Mössbauer spectroscopy,

TABLE II. The lattice parameters of Fe_2YZ were determined at room temperature and are given for an fcc lattice. Left are shown the lattice parameters of Fe_2YZ annealed at 673 K and right at 1173 K, and * marks those cases which have involved decomposition of the sample.

Compound	a (Å)	a (Å)
Fe_2CoGe	5.78	5.76
Fe_2CuGa	5.86	5.86
Fe_2NiGa	5.81	*
Fe_2NiGe	5.76	5.76
Fe_2CuAl	5.83	*

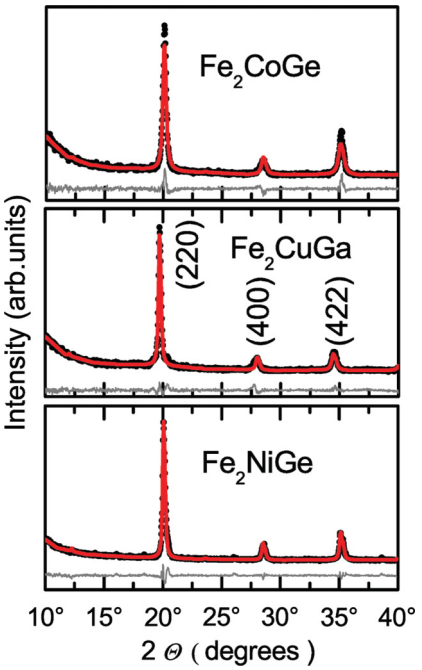

FIG. 4. (Color online) XRD of Fe_2CoGe, Fe_2CuGa, and Fe_2NiGe alloys annealed at 1173 K. The diffraction patterns are compared to the results of Rietveld refinements.

which is a local probe technique. The results obtained with this technique will be presented below.

C. Characterization of magnetic properties

As displayed in Fig. 5, all compounds exhibit soft ferromagnetism. It is noted that the magnetic behavior slightly depends on the annealing temperature. The isothermic magnetization curves at 5 K are essentially saturated in an induction field of 5 T. The magnetic moments at 5 K and 5 T together with the magnetic ordering temperatures T_C are summarized in Table III. The latter have been derived from the drop in the

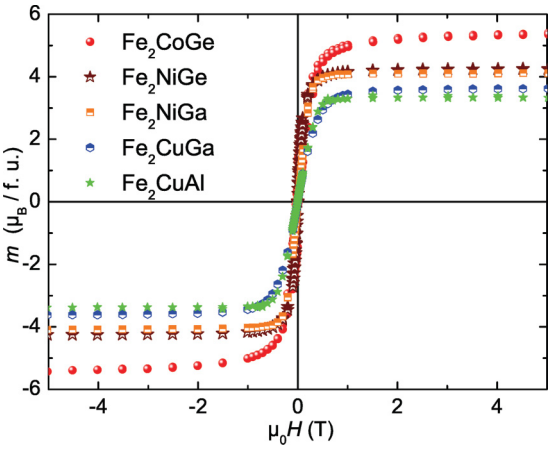

FIG. 5. (Color online) Field-dependent magnetization m per formula unit of Fe_2YZ compounds annealed at 673 K and measured at 5 K.

temperature-dependent magnetization curves measured at 0.1 or 1 T (Fig. 6). Additional anomalies in the T dependence of Fe_2NiGe and Fe_2CuAl point to the ordering of a minority phase in these samples. The valence electron concentration (VEC) per formula unit and magnetic moments obtained from electronic structure calculations are included in Table III, too. All materials considered in this paper contain 29 or 30 valence electrons per formula unit. The magnetic moment of the 673-K annealed sample of Fe_2CoGe is somewhat larger than the value of $5.1\mu_B$ reported earlier,[15] while that of the 1173-K sample is in better agreement with the published data. The experimental magnetic moments of Fe_2CoGe are quite close to the value of $5\mu_B$ expected from the generalized Slater-Pauling (SP) rule, which predicts the magnetic moment m per formula unit given in μ_B for half metallic X_2YZ phases as $m = \text{VEC} - 24$ with $\text{VEC} = 29$ for Fe_2CoGe. This suggests that Fe_2CoGe could be a half metallic ferromagnet, however, the spin polarization appears to be not complete[15](see also Sec. III). The magnetic moments of all the other materials

TABLE III. Summary of the magnetic properties (magnetic moments m, Curie temperatures T_C) of Fe_2YZ alloys obtained from experiment (SQUID and Mössbauer measurements, left part of the table) and from *ab initio* electronic structure calculations (right part of the table, indicated with m_{th}). The total magnetic moments m per formula unit are obtained from magnetization measurements at 5 K, whereas the magnetic moments at the Fe sites are derived from room temperature Mössbauer spectra.

Compound	VEC[a]	m[b] (μ_B)	T_C[b] (K)	m[c] (μ_B)	m [FeA][d] (μ_B)	m[FeB][d] (μ_B)	m_{th}[e] (μ_B)	m_{th}[FeA][e] (μ_B)	m_{th}[FeB][e] (μ_B)
Fe_2CoGe	29	5.40	925	5.0	2.6	1.6	5.15	2.68	1.51
Fe_2NiGe	30	4.29	750	4.46	2.5	1.7	4.47	2.53	1.67
Fe_2NiGa	29	4.20	845			2.05[f]	4.81	2.64	1.82
Fe_2CuGa	30	3.60	798	3.40	2.5	1.7 2.1[g]	4.04	2.34	1.78
Fe_2CuAl	30	3.30	875		2.2	1.7	3.80	2.23	1.67

[a]VEC is the valence electron concentration.
[b]Measurement for the 673-K annealed sample.
[c]Measured for the sample annealed at 1173 K.
[d]Estimated from the Mössbauer hyperfine fields of the 673-K annealed sample at room temperature.
[e]Theoretical moments for the fully ordered inverse cubic Heusler phase calculated for the experimental lattice parameters.
[f]Derived from average H_{hf} value of the Mössbauer hyperfine pattern.
[g]Derived from the average H_{hf} value of the broad component in the Mössbauer hyperfine pattern.

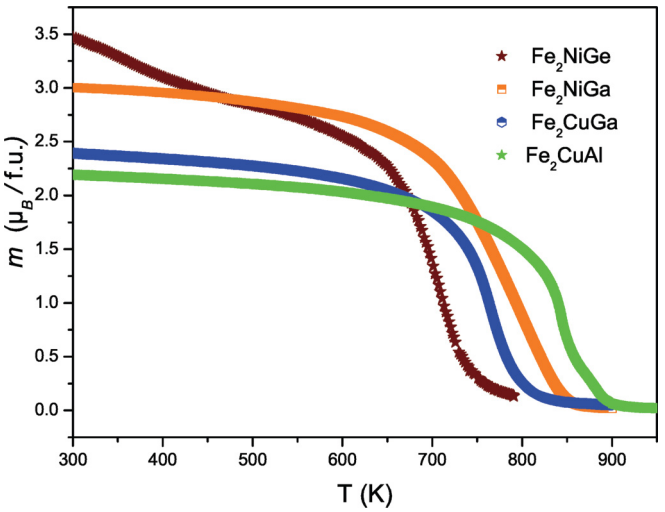

FIG. 6. (Color online) Temperature-dependent magnetization m per formula unit of Fe_2YZ alloys annealed at 673 K. The measurements were performed in the range 300–900 K at 0.1 T (for Fe_2CuAl, Fe_2CuGa, Fe_2NiGa, Fe_2CoGe) and 1 T (for Fe_2NiGe) induction fields.

do not follow the generalized SP rule. The magnetic ordering temperatures are quite high ($T_C > 700$ K) which makes the materials suitable for potential applications. A detailed comparison of experimental magnetic moments from both bulk magnetization and Mössbauer measurements with theoretical moments will be compiled in Sec. III.

D. Mössbauer measurements

The potential of Mössbauer spectroscopy for studying the degree of atomic order in iron-containing Heusler compounds has been demonstrated previously for the series $Co_{2-x}Fe_{1-x}Si$ (Ref. 27) and $Co_2Mn_{1-x}Fe_xAl$.[28] The former compounds crystallize in well-ordered cubic Heusler structures which evolve from the regular $L2_1$ structure for Co_2FeSi to the inverse X structure for Fe_2CoSi. The Mössbauer spectra of $Co_{2-x}Fe_{1-x}Si$ ($0.1 \leqslant x \leqslant 0.9$) are composed of two sharp six-line patterns with magnetic hyperfine fields H_{hf} in the range 320–340 kOe (sextet A) and 185–195 kOe (sextet B), respectively. The successive replacement of Co by Fe atoms in $Co_{2-x}Fe_xSi$ leads to a corresponding increase in the area fraction of sextet B. From the above-mentioned series it can be concluded unambiguously that the A sextet corresponds to Fe sites with $(8-4x)$ Co and $4x$ Fe atoms in the first coordination sphere, the B sextet corresponds to Fe sites with four Fe(A) and four nonmagnetic Si neighbors, independent of x. The variation in the H_{hf} values of the two sites due to the substitution is quite small. In the $L2_1$ structure of Co_2FeSi the Fe(A) atoms have O_h symmetry with eight Co nearest neighbors and six Si atoms in the second coordination shell. In the final member compound Fe_2CoSi all atoms have T_d symmetry and the Fe(A) sites are surrounded by four Fe(B) and four Co atoms. On the other hand a $B2$-type disorder in the series $Co_2Mn_{1-x}Fe_xAl$ gives rise to a strongly broadened hyperfine pattern which reflects the superposition of Fe sites in different coordination environments. A detailed analysis of these spectra has been given in Refs. 27 and 29. The Mössbauer spectra demonstrating the hyperfine field distribution at room

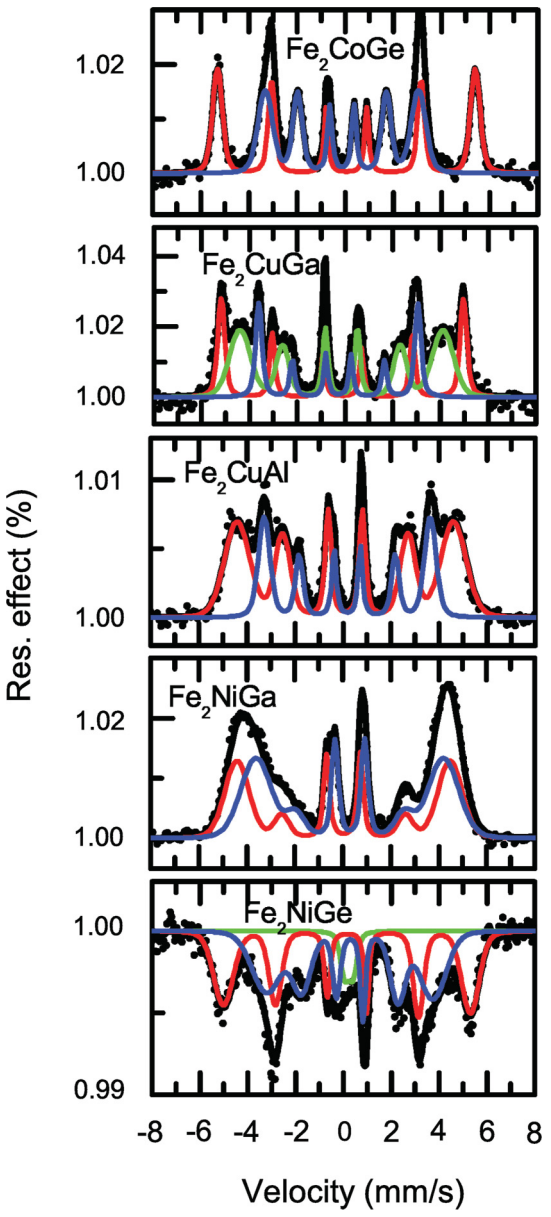

FIG. 7. (Color online) Mössbauer spectra of the Fe_2YZ samples annealed at 673 K. The spectrum of Fe_2NiGe is a transmission spectrum, the others are backscattering spectra. The experimental points are shown as black dots, fitted by the black solid line (total signal). The total signal is decomposed into two (or three) distinct contributions (red, blue, and green, respectively), each corresponding to a certain environment of the Fe atoms.

temperature (RT) for the present Fe_2YZ materials annealed at 673 K are shown in Figs. 7 and 8. The transmission and backscattering spectra in Fig. 7 are representative for the bulk materials and will be discussed in detail below. The more surface sensitive conversion electron Mössbauer (CEM) spectra (Fig. 8) reveal additional line broadening and the details seen in the backscattering or transmission spectra are lost. This points to enhanced disorder in the surface layers. Also Mössbauer spectra of the samples annealed at 1173 K were recorded. As there was no improvement of atomic order in any of the samples and according to XRD even partial

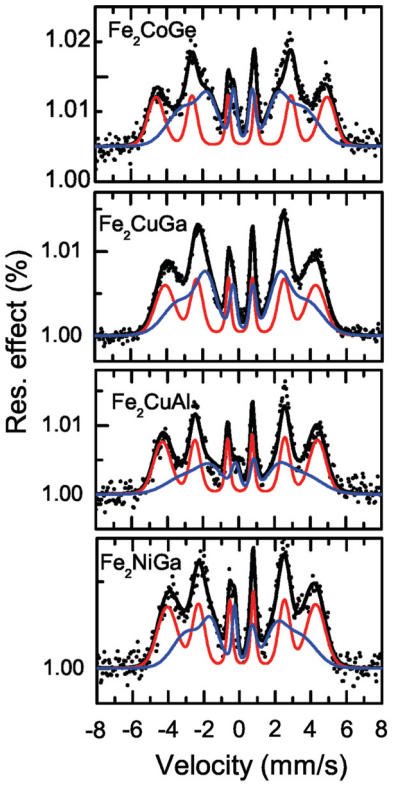

FIG. 8. (Color online) Conversion electron Mössbauer spectra of Fe_2YZ samples annealed at 673 K and measured at RT. The experimental points are shown as black dots, fitted by the black solid line (total signal). The total signal is decomposed into two distinct contributions (red and blue, respectively), each corresponding to a certain environment of the Fe atoms.

decomposition occurred for Fe_2NiGa and Fe_2CuAl, we restrict the discussion to the 673-K annealed samples. All data were fitted with a Voigt profile model which yields a distribution of hyperfine fields. Actually this approximates the superposition of local coordination environments as has been exemplified in more detail in Ref. 28.

The values of the Mössbauer parameters of Fe_2YZ obtained from the data evaluation for bulk samples are summarized in Table IV. All spectra can be described by two or three hyperfine sextets which show that the corresponding materials are magnetically ordered at room temperature. The detailed spectral shapes differ, however, which suggests a varying degree of disorder within the series of compounds. The Mössbauer spectra and H_{hf} values of Fe_2CoGe are close to those of $Co_{2-x}Fe_{1+x}Si$,[27] with two well-defined sextets. Thus, the sextet with higher H_{hf} is assigned to Fe(A) sites and the second sextet with lower H_{hf} value to the Fe(B) sites. The intensity ratio of the two sextets is approximately 1:1. Since the two Fe atoms in inverse Heusler Fe_2YZ phases adopt two different lattice sites, see Fig. 1, these data evidence that Fe_2CoGe like Fe_2CoSi crystallizes in the inverse Heusler (X) structure. Mössbauer spectra not only give information about the atomic distribution over the crystallographic sites but also allow an estimation of the ordered magnetic moments for Fe atoms at the A and B sites, respectively. In cubic or nearly cubic compounds the internal magnetic hyperfine field

TABLE IV. Mössbauer parameters at room temperature of Fe_2YZ samples annealed at 673 K. H_{hf} denotes the hyperfine field, IS the isomer shift, and A is the relative area fraction. The maximum errors in H_{hf}, A, and IS were ± 4 kOe, ± 3%, and ± 0.02 mm/s, respectively.

	T_{anneal} = 673 K		
Sample	H_{hf} (kOe)	A (%)	IS (mm/s)
Fe_2CoGe	332	48	0.05
	197	52	−0.14
Fe_2CuGa	314	28	−0.11
	264	49	−0.15
	207	22	−0.27
Fe_2NiGa	275	44	0.04
	242	56	0.30
Fe_2NiGe	320	44	0.15
	216	51	0.27
Fe_2CuAl	279	67	0.10
	214	33	0.18

is determined by the Fermi contact term, which arises from the polarization of the s-electron density at the nucleus. It has been shown that H_{hf} scales linearly with the magnetic moments determined from neutron or magnetization studies.[30] Taking a slope of 125 kOe/μ_B for Fe germanides from Ref. 30 one roughly estimates the magnetic moments as ∼2.6μ_B and ∼1.6μ_B for Fe(A) and Fe(B) atoms in Fe_2CoGe, respectively. Considering the total magnetic moment of 5.4μ_B from the magnetization studies (at 5 K) the remaining Co moment must be about 1.1μ_B in the case of ferromagnetic ordering. These estimates are in fair agreement with the calculated moments of 2.7μ_B and 1.4μ_B for the Fe sites and 0.9μ_B for the Co sites reported in Ref. 15. As for all the present materials, the Curie temperatures are above 700 K and the estimates of the moments from the room temperature Mössbauer spectra can be used for comparison with theoretical results. These data are included in Table III. Quite similar spectra are observed for Fe_2NiGe. Accordingly, also Fe_2NiGe essentially crystallizes in the inverse Heusler structure but line broadening for both subspectra and the small deviation from the ideal intensity ratio of 1:1 indicate some disorder. In case of Fe_2NiGe, from the H_{hf} values (see Table IV) one estimates the magnetic moments as 2.5μ_B and 1.7μ_B for the Fe(A) and Fe(B) atoms, respectively. The sum of the moments nearly corresponds to the total magnetic moment of 4.3μ_B for Fe_2NiGe obtained from magnetometry, which suggests that the Ni sites do not contribute much to the magnetic ordering. It is noted, however, that the present material is not completely single phase. The Mössbauer spectrum reveals a 6% contribution of a paramagnetic quadrupole doublet (IS = 0.23 mm/s, ΔE_Q = 0.37 mm/s). In agreement with the clues from the XRD patterns this signal is assigned to an Fe_xGe_y impurity as the magnetic behavior of this system is known to depend strongly on the Fe-Ge ratio.[30]

In contrast to Fe_2CoGe and Fe_2NiGe the Mössbauer spectrum of Fe_2NiGa reveals enhanced disorder. The two subspectra are no longer resolved and the spectra were modeled by a superposition of two broad sextets the average H_{hf} values of which are only slightly different. Hence, the distinction

between well defined A and B sites is not meaningful. The disorder in Fe_2NiGa leads to a pronounced distribution of hyperfine fields and of the corresponding magnetic moments over various sites with differing local coordination environment. The nearly structureless spectra may point towards an $A2$-type disorder where alloying occurs between all sites. The average H_{hf} of 255 kOe roughly corresponds to an ordered moment of $2\mu_B$ per Fe or $4\mu_B$ per formula unit which is close to the total moment of about $4.2\mu_B$. The considerable disorder in Fe_2NiGa is also suggested by the XRD pattern which reveals a pronounced broadening of the (400) and (422) reflections. Additional information about the orientation of the magnetic moments can be derived from the intensities of the Fe_2NiGa spectrum. As it is well known[31] for ^{57}Fe, in the case of no or small quadrupole interaction only six lines of the eight possible transitions in a magnetic field are observed with the intensity ratio $3 : Z : 1 : 1 : Z : 3$. The Z value is characteristic for the relative intensity of the $\pm\frac{1}{2} \longrightarrow \pm\frac{1}{2}$ transitions and depends on the angle θ between the propagation vector of the γ radiation and the direction of H_{hf}: $0 \leqslant Z \leqslant 4$. For a random orientation (powder) and thin absorbers $Z = 2$, whereas $Z = 4$ for $\theta = 90^\circ$ and $Z = 0$ for $\theta = 0^\circ$, respectively. Preferred orientation of crystallites accordingly leads to deviation from the ideal powder value $Z = 2$. The backscattering spectrum of Fe_2NiGa (Fig. 7) reveals a strongly diminished relative intensity of the second and fifth lines which suggests that the magnetization occurs essentially along the direction of the γ beam, i.e., perpendicular to the sample surface.

Well ordered and disordered regions appear to coexist in the sample of Fe_2CuGa. The spectra of Fe_2CuGa are best described by two sharp and an additional broad sextet. The H_{hf} values and thus also the magnetic moments of the sharp features are very similar to those of Fe_2NiGe. These signals are attributed to Fe(A) and Fe(B) sites in well ordered domains of the material with X structure. The broad feature is assigned to domains with strong disorder. The average H_{hf} of 265 kOe corresponds just to the average of the H_{hf} values of the A and B sites. Accordingly, although the distribution of the moments is changed in the course of the disorder the average magnetic moment ($4.2\mu_B$ per formula unit) nearly remains the same. This is in agreement with the observation that the total magnetic moments in Heusler compounds frequently are not changed much by disorder. Similar spectral shapes are also obtained for Fe_2CuAl. The spectra have been approximated by two hyperfine sextets. The sharp sextet with $H_{hf} = 214$ kOe is assigned to Fe(B) sites with regular coordination geometry (4 Fe and 4 Al neighbors). Its intensity contribution (33%) is, however, smaller than for an ideal inverse Heusler phase. The broad second sextet thus accounts for a superposition of Fe sites with differing environment due to disorder. As in other Al containing Heusler compounds a pronounced $B2$-type exchange between Fe and Al sites is expected to contribute to the disorder.[28] Antisite disorder between the Fe(B) and Al sites is possibly the origin for an enhanced intensity contribution of Fe(A)-like signals as Fe atoms at Al sites are in a similar environment as Fe(A) atoms. There is no clear evidence of an Fe-based impurity in the spectrum of Fe_2CuAl although an impurity phase was detected in the XRD pattern. This is in accord with the clue from the XRD data that the impurity corresponds to a Cu_xAl_y phase.

Having established the typical features of the Mössbauer spectra for the present materials we now discuss the results with respect to the theoretical predictions of Ref. 14. For Fe_2CoGe the inverse cubic Heusler structure was obtained as the most stable one. This is in agreement with the Mössbauer spectra of Fe_2CoGe which show two well-defined Fe sites. For all the other materials, however, the structure predictions are contradicted by the Mössbauer spectra. In Ref. 14 an inverse Heusler structure was suggested for Fe_2NiGa. In contrast, the Mössbauer spectrum of Fe_2NiGa does not reveal the typical pattern of the inverse Heusler structure. The broad features rather point towards a strongly disordered arrangement of the atoms. In case of Fe_2NiGe, Fe_2CuGa, and Fe_2CuAl the inverse Heusler structure was shown to be more stable than the regular one, but it was suggested that there is an inherent tendency for a structural distortion. Hence, it was predicted that the regular tetragonal Heusler structure becomes more stable for these materials. As it has been shown already in Sec. II B, there is no sign of a tetragonal distortion in any of the present XRD patterns. The Mössbauer spectrum suggests that it is essentially the inverse Heusler structure which is adopted by Fe_2NiGe. Also the spectra of Fe_2CuGa and Fe_2CuAl show signatures of the inverse Heusler structure, however, pronounced disorder is apparent from the spectra too. Furthermore, there is no indication of quadrupole interactions in the Mössbauer spectra which would be expected for tetragonal Heusler phases.

Finally, we mention that we have tried to synthesize Fe_2ZnAl, which has also been predicted as a regular tetragonal Heusler phase[14] with a magnetic moment of $\sim 4\mu_B$. However, analysis of the Mössbauer spectra and XRD data of a sample with nominal composition Fe_2ZnAl revealed the presence of a nonmagnetic component which was identified as FeAl. An additional magnetic component, the fraction of which increases from 10% in the 673 K annealed sample to 55% in the 1173 K sample presumably corresponds to Fe_3Al. Thus, the stabilization of a Heusler phase was not successful in this case.

III. RESULTS OF THE ELECTRONIC STRUCTURE CALCULATIONS

In order to gain more insight into the atomic and electronic structure and magnetism of the Fe_2YZ compounds, we have performed *ab initio* electronic structure calculations based on density-functional theory (DFT). All calculations were carried out by using the fully relativistic Korringa-Kohn-Rostoker (KKR) Green's-function method as implemented in the SPR-KKR package.[32] The exchange and correlation were treated by the Vosko-Wilk-Nusair form of the local-density approximation (LDA).[33]

The lattice parameters were taken from the experimental data (see Table II). The primitive unit cell contains four atoms in the lattice with the Wyckoff positions A (0, 0, 0), B ($\frac{1}{4}$, $\frac{1}{4}$, $\frac{1}{4}$), C ($\frac{1}{2}$, $\frac{1}{2}$, $\frac{1}{2}$), D ($\frac{3}{4}$, $\frac{3}{4}$, $\frac{3}{4}$). In the regular Heusler structure the B and D positions are equivalent due to inversion symmetry, whereas in the case of the inverse Heusler structure these sites become inequivalent (see Fig. 1). In the case of the fully ordered Fe_2YZ inverse Heusler compounds sites A and B are occupied by Fe, which we will refer to as Fe(A) and Fe(B) site, respectively. Since the Mössbauer measurements have clearly shown that the Heusler compounds in the Fe_2YZ series show

a certain degree of chemical disorder, we have considered the antisite disorder by using the so-called coherent potential approximation (CPA).[20,21] In the following we will consider the cubic Heusler phases including the effects of disorder and nonstoichiometry.

A. Fe_2CoGe

To check whether the methodology presented above is suitable for the description of structural and magnetic properties of the Fe_2YZ materials, first we have performed a set of calculations for Fe_2CoGe and compared the results with the data already available from the literature.[15] We have considered four different model systems in the cubic structure, where the site occupations were selected with the following configurations: (a) fully ordered Heusler structure; (b) chemically disordered structure (50% of Fe is mixed with Co); (c) chemically disordered inverse Heusler phase (50% of the Fe sitting in position C mixed with Co); (d) a fully ordered inverse Heusler structure. We found that the structure stability increases from (a) to (d). The configurations (b) and (c) are isoenergetic, sitting by 285 meV (per formula unit) lower than the ordered regular Heusler structure (a). Finally, the most stable phase appears to be the fully ordered inverse Heusler phase by about 30 meV lower energy compared to (b) and (c). Thus, the ordered regular $L2_1$ structure is unstable, and although disorder increases the stability, the most stable phase has the ordered inverse Heusler structure.

This is in good agreement with the experimental results, which suggest that Fe_2CoGe crystallizes as an inverse Heusler compound with a rather small amount of antisite disorder. For Fe_2CoGe in the X structure the computed total magnetic moment of $5.15\mu_B$ is in reasonable agreement with the experimental values of 5.0–$5.4\mu_B$ (see Table III and Ref. 15). The calculated local moments are: $2.68\mu_B$, $1.51\mu_B$, and $1.01\mu_B$ on Fe(A), Fe(B), and Co, respectively. These computed values agree with the Fe moments of $2.6\mu_B$ and $1.6\mu_B$ derived from the Mössbauer spectrum of Fe_2CoGe. The present results are comparable with the calculations of Ref. 15 which report the moments of $2.74\mu_B$, $1.38\mu_B$, and $0.94\mu_B$ on Fe(A), Fe(B), and Co sites, respectively. By assuming the ferromagnetic order, one derives from the Mössbauer data and the measured magnetization of $5.4\mu_B$ the local moment of Co as $1.1\mu_B$, in agreement with the present calculations. As it follows from the calculated density of states (DOS) for the ordered inverse Heusler structure (see Fig. 9) Fe_2CoGe is not a half metallic ferromagnet (which is also clear from Ref. 15).

B. Fe_2NiGe

The EDX data (see Table I) for Fe_2NiGe indicate that the sample is slightly off stoichiometric, with a small portion of Fe (about 2.5%) substituted by Ni. The line shape of the Mössbauer spectrum suggests that the sample essentially remains ordered, but in the structure there is a certain amount of disorder present. So, for Fe_2NiGe we have theoretically investigated nine different scenarios in the inverse Heusler structure. First we have looked at the stoichiometric compound, where we considered (a) the fully ordered inverse Heusler structure; (b) antisite disorder between Fe(A) and Ni, where 6% of Fe was substituted with Ni; (c) antisite disorder between Fe(B) and Ni, where 6% of Fe was substituted with Ni; (d) 6% substitution of Fe(A) with Ge; (e) 6% substitution of Fe(B) with Ge. We have also studied the off-stoichiometric compositions, where the model systems were created via (f) removal of 3% of Fe from site A; (g) removal of 3% of Fe from site B; (h) 3% substitution of Fe(A) by Ni; (i) 3% sustitution of Fe(B) by Ni.

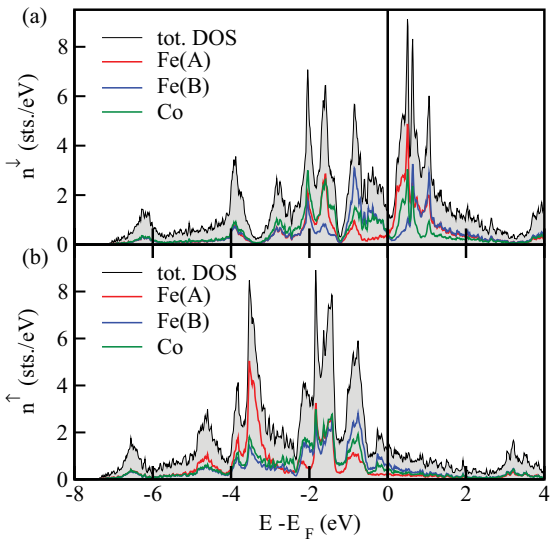

FIG. 9. (Color online) Spin resolved and atom projected DOS of Fe_2CoGe, where (a) and (b) panels correspond to the minority and majority spin channels, respectively. The red, blue, and green curves refer to Fe(A), Fe(B), and Co contributions. The total DOS is shown by a gray shaded area.

Indeed, calculations indicate that the fully ordered inverse Heusler structure is not the most stable configuration for Fe_2NiGe. Instead, the Fe-Ni antisite disorder leads to more stable structures. Namely, the compositions (b) and (c) are lower in energy compared to configuration (a) by 6 and 8 meV per formula unit, respectively. In contrast to the Fe-Ni, the Fe-Ge exchange is energetically unfavorable for each of the Fe sites: compositions (d) and (e) are higher in energy by about 65 and 150 meV per formula unit compared to the fully ordered case.

Still, these small energy differences between subsequent structures are comparable with the average thermal energy of the atoms at the annealing temperature, indicating that the detailed annealing conditions can control the nature of the disorder in the Fe_2YZ inverse Heusler phases. The energy of configuration (f) is found to be 15 meV lower than (g), indicating that the creation of Fe point defects in position (A) is more likely than in position (B).

If 3% of Fe is substituted by an additional 3% of Ni, the structures (h) and (i) are isoenergetic, i.e., in this specific case from the perspective of the total energy the system is not biased towards Fe(A) or Fe(B) sites. This means that with slight Ni excess, Fe atoms are randomly removed both from positions A and B, and the empty sites are being occupied with Ni. The spin-resolved and atom-projected DOS computed for the fully ordered stoichiometric Fe_2NiGe in the inverse Heusler structure is shown in Fig. 10. For the inverse Heusler phase the calculated total moment is

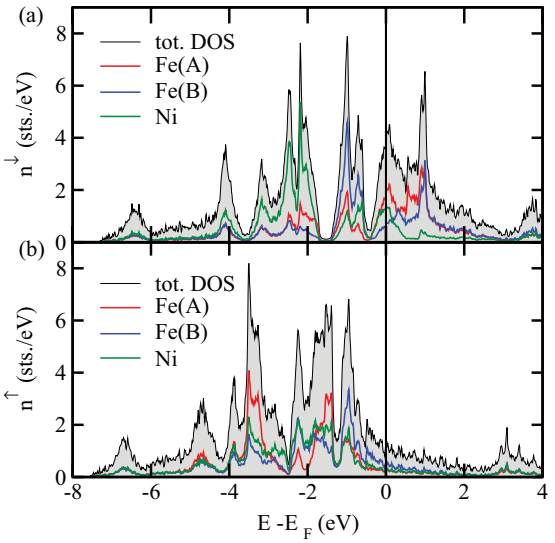

FIG. 10. (Color online) Spin resolved and atom projected DOS of Fe_2NiGe, where panels (a) and (b) correspond to the minority and majority spin channels, respectively. The contributions of Fe(A), Fe(B), and Ni are represented with red, blue, and green curves. The total DOS is shown by a gray shaded area.

$4.47\mu_B$ per formula unit, which agrees with the experimental moments of $4.29\mu_B$ or $4.46\mu_B$ measured for the samples with SQUID magnetometry. The computed local moments on Fe(A), Fe(B), and Ni atoms are $2.53\mu_B$, $1.67\mu_B$, and $0.29\mu_B$ respectively. The Fe local moments agree with those derived from Mössbauer measurements: $2.5\mu_B$ and $1.7\mu_B$ for the Fe(A) and Fe(B) sites. Similar behavior was found for the disordered structures (b)–(e) corresponding to the stoichiometric composition.

In cases (h) and (i) in which Fe was substituted by Ni, corresponding to the composition measured via EDX, the calculated total moments were $4.39\mu_B$ and $4.42\mu_B$, respectively. For structures (f) and (g), where 3% of Fe is missing (no additional Ni present), the total moments were $4.38\mu_B$ and $4.43\mu_B$, respectively. For those cases which resemble the experimental composition, the respective local moments were $2.52\mu_B$, $1.68\mu_B$, and $0.31\mu_B$ for configuration (i) and for structure (h) $2.54\mu_B$, $1.67\mu_B$, and $0.29\mu_B$ for Fe(A), Fe(B), and Ni, respectively.

Thus, a small amount of disorder, Fe deficiency, or Ni excess do not change considerably the magnetic properties of Fe_2NiGe in the inverse Heusler structure.

C. Fe_2NiGa

In the case of Fe_2NiGa the experimental results presented in the previous section have pointed out that the material exhibits a rather strong degree of disorder. To sample the potential atomic arrangement in the disordered phase, we have carried out calculations on 11 model systems each having a stoichiometric composition.

The first scenario was the ordered inverse Heusler structure, which served as the reference. For the fully ordered structure we have calculated a magnetic moment of $4.81\mu_B$, which is about $0.6\mu_B$ higher than the experimentally measured value of $4.20\mu_B$.

Next we have looked into the effect of antisite disorder upon the magnetization and energetics of Fe_2NiGa between Fe(A) and Fe(B) and Ni and Ga for stoichiometric compositions. We found that by exchanging the site occupation of Fe(A) with 10%, 20%, and 50% of Ni, the structures generated hereby are higher in energy by about 14, 15, and 89 meV per formula unit, respectively, compared to the ideal inverse Heusler phase. This indicates that a small amount of Fe(A) (up to about 10–20%) can be exchanged by Ni rather easily.

In contrast to this, if one exchanges 50–60% of Fe(B) with Ni, the structure with Fe(B)-Ni antisite disorder becomes more stable by about 9 meV per formula unit than the ordered phase. Thus, in case of Fe_2NiGa the ground state does not correspond to the fully ordered inverse Heusler phase. For the lowest energy configuration the calculated total moment is $4.77\mu_B$, where the local moments on Fe(A), Fe(B), and Ni are $2.65\mu_B$, $1.86\mu_B$, and $0.33\mu_B$, respectively. Thus, the magnetic moment of this structure is still higher than the SQUID data by about $4.2\mu_B$ per unit cell.

Also the average moment on the Fe sites of $2.25\mu_B$ is somewhat higher than the average moment of $2.05\mu_B$ estimated from the broad sextets in the Mössbauer spectrum. Upon exchanging either Fe(A) or Fe(B) with Ga the disordered structures were all unstable relative to the reference case independent of the Fe position. The total magnetic moments of the systems with Fe-Ni and Fe-Ga exchange are computed in the range $5.03–4.59\mu_B$.

Due to the fact that the Mössbauer spectra may suggest random alloying, we have also considered the case of an $A2$-type structure, where the constituent atoms are randomly distributed on all four lattice sites. The calculations have shown that such an $A2$-type random structure where all atoms are coupled ferromagnetically is rather unstable, by about 440 meV per formula unit compared to the reference, which is the ordered inverse Heusler phase.

D. Fe_2CuGa

For the Fe_2CuGa sample the experiment reveals both well-ordered and disordered regions. Since the ordered regions should correspond to the ideal ferromagnetic inverse Heusler structure, we have first investigated this configuration. The corresponding spin-resolved and atom-projected DOS is shown in Fig. 11. The calculated total magnetic moment of $4.04\mu_B$ is somewhat larger than the experimental one ($3.6\mu_B$) derived from the SQUID measurements. The origin of this small discrepancy cannot be resolved unambiguously, however, the experimental moment may be too small due to the presence of the minor impurity phase as suggested by the XRD pattern. On the other hand, the calculated local moments of $2.34\mu_B$ for Fe(A) and $1.78\mu_B$ for Fe(B) sites agree with the corresponding values of $2.5\mu_B$ and $1.7\mu_B$ derived from the sharp features in the Mössbauer spectrum. The moments on the Cu and Ga sites are negligibly small.

To gain new insights via CPA on the potential nature of the disordered phase, we have carried out calculations for six configurations taking into account various kinds of Fe-Cu and Fe-Ga antisite disorder. The calculations indicate that 50% of Cu-Fe(A) exchange leads to a more stable structure compared to the fully ordered inverse Heusler structure with a

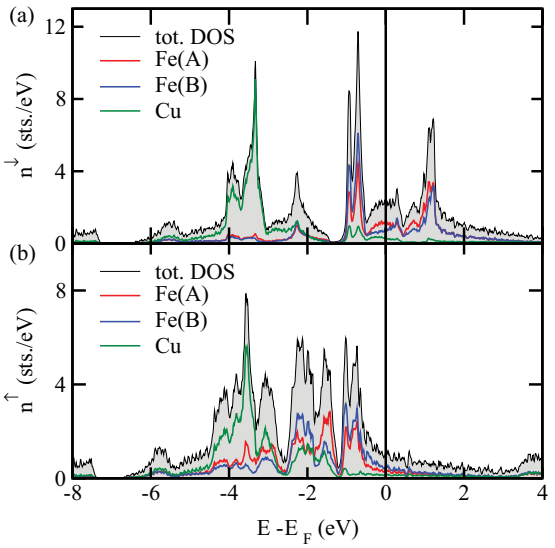

FIG. 11. (Color online) Spin resolved and atom projected DOS of Fe_2CuGa. Panels (a) and (b) correspond to the minority and majority spin channels, respectively. The contributions of Fe(A), Fe(B), and Cu are shown with red, blue, and green curves, respectively, and the total DOS is shown by a gray shaded area.

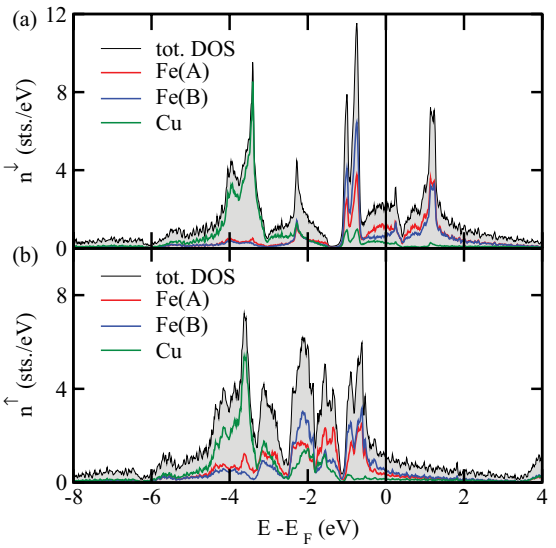

FIG. 12. (Color online) Spin resolved and atom projected DOS of Fe_2CuAl, where (a) and (b) panels correspond to the minority and majority spin channels, respectively. The red, blue, and green curves refer to Fe(A), Fe(B), and Cu contributions. The total DOS is shown by a gray shaded area.

stabilization energy of 71 meV per primitive unit cell. Besides this, we found that an even more stable configuration can be created via chemical disorder, where alloying is present between Fe and Cu, with 18%, 44%, and 44% of Fe-Cu antisite exchange on Wyckoff positions A, B, and D, respectively. This structure is 110 meV lower in energy compared to the ideal ordered inverse Heusler structure, which indicates that the system might undergo a spontaneous mixing between Fe and Cu, giving rise to the appearance of a broad sextet seen in the Mössbauer spectra. For the systems with Fe-Cu disorder the total magnetic moments assuming ferromagnetic ordering have been calculated to be in the range 4.29–4.31μ_B, where the local moments were 2.48μ_B, 1.95μ_B, and 1.94μ_B for Fe(A), Fe(B), and Fe(D), respectively. The average value of 2.1μ_B over these sites is in good agreement with the average moment of 2.1μ_B estimated from the hyperfine field value of the broad sextet.

Next we considered the effect of Fe-Ga disorder, which has shown that even a small amount of Fe-Ga antisites is energetically unfavorable. For 10% of antisite disorder on Fe(A) or Fe(B) sites the structures were less stable, by about 30 and 85 meV per formula unit, respectively, compared to the ordered inverse Heusler structure. This indicates that Fe-Ga antisite disorder in Fe_2CuGa is less likely to happen than Fe-Cu alloying. The calculated total moments in the case of Fe-Ga antisite disorder are in the range 4.15–4.25μ_B which are only slightly enhanced compared to the ideal X structure.

E. Fe_2CuAl

For the Fe_2CuAl sample it was found experimentally that the sextet assigned to Fe(B) in the Mössbauer spectra has a lower intensity than it should have in the ordered inverse Heusler phase, indicating that there is a certain amount of disorder involved. Also, there is a second broad sextet with enhanced relative intensity present, pointing towards different local Fe coordination environments. These spectral features suggest an inverse Heusler structure, where Fe(B)-Al antisite disorder leads to an enhanced fraction of Fe(A)-like sites. We have first investigated the ideal X phase of Fe_2CuAl theoretically, for which the computed total DOS and atom projected DOS is shown in Fig. 12. The calculated total moment of 3.80μ_B considering ferromagnetic ordering is somewhat higher than the measured value of 3.3μ_B. The experimental value may, however, be too small as there is an impurity phase evident in the XRD pattern. Similar to the case of Fe_2CuGa the local moments deduced from the Mössbauer spectra on Fe(A) and Fe(B) sites of 2.2μ_B and 1.7μ_B are in a real good agreement with the calculated local moments of 2.23μ_B and 1.67μ_B. This confirms that Fe_2CuAl basically crystallizes in a cubic inverse Heusler structure. Further, we studied the effects of Fe-Cu or Fe-Al antisites. Up to 30% of Fe-Cu antisite exchange the structure is more stable by about 12 meV per formula unit compared to the ideal inverse structure, and going above 30% the structure becomes less stable by about around 15 meV.

By exchanging Fe with Al the calculations show that the structures generated are practically isoenergetic with the ordered inverse Heusler structure. This result agrees with the experimental observations from Ref. 28. The total moments for configurations with Fe-Cu and Fe-Al disorder are in the range 3.91–3.96 and 3.80–3.81μ_B, respectively, which is similar as in the case of the fully ordered Heusler phase. Thus, the calculations indicate that although there is a slight bias towards the Fe-Cu antisite disorder, in Fe_2CuAl the spontaneous formation of both Fe-Cu- and Fe-Al-type disorder is highly likely. As it follows, in many cases the antisite disorder does not change radically the magnetic properties of the Heusler compounds.

F. Fe_2ZnAl

Finally we considered the case of Fe_2ZnAl (predicted theoretically[14]). We have investigated the hypothetical inverse cubic Heusler structure, and found that the calculated total moment of $3.27\mu_B$ is nearly twice larger than the experimental moment of a sample with the nominal composition Fe_2ZnAl. Such significant discrepancy suggests that the sample is not a Heusler phase. In fact, the XRD and Mössbauer data revealed that in the mixed-phase samples nonmagnetic FeAl, in addition to Fe_3Al, were the major iron-based components.

IV. CONCLUSIONS

We have synthesized and characterized the new iron-based Heusler phases Fe_2NiGe, Fe_2CuGa, and Fe_2CuAl, the existence of which has been suggested by previous theoretical work.[14] In addition we have investigated in more detail the known compounds Fe_2CoGe and Fe_2NiGa. The newly synthesized Fe_2YZ phases were predicted to adopt a regular tetragonal Heusler structure, whereas the present experimental results revealed that the materials basically crystallize in the cubic inverse Heusler (X) structure with differing degrees of atomic disorder. For these Fe-based materials ^{57}Fe Mössbauer spectroscopy is a very useful local-probe technique to unravel the atomic disorder and to estimate the magnetic moments at the iron sites. All the compounds are soft ferromagnets with Curie temperatures up to about 900 K which makes them suitable for potential magnetic applications. The electronic structures of the materials have been studied by *ab initio* DFT calculations including the effects of disorder and nonstoichiometry within the CPA approximation. The good agreement between calculated and experimental magnetic moments at the Fe sites is further support that the compounds basically adopt the cubic inverse Heusler structure. Atomic disorder which is apparent in the experimental data leads to further stabilization of the cubic structure without changing the magnetic properties too much. The case of Fe_2NiGa, which was predicted to crystallize in the cubic X structure is not completely clear yet. Both XRD and Mössbauer data evidence an increased atomic disorder and the calculated magnetic moments are somewhat higher than the experimental ones. Attempts to synthesize Fe_2ZnAl, a further phase which was also suggested to adopt the tetragonal Heusler structure,[14] were unsuccessful. While there is a good consistency between the present experimental and theoretical results for the cubic inverse Heusler Fe_2YZ materials it remains to be clarified why Fe_2NiGe, Fe_2CuGa, and Fe_2CuAl do not adopt the tetragonal structures predicted previously.

ACKNOWLEDGMENTS

We thank G. Klingelhöfer for the possibility to use the MIMOS spectrometer, M. Blumers for his support, and G. H. Fecher for helpful discussions. Financial support by the Deutsche Forschungsgemeinschaft (Project P2.3-A of research unit FOR 1464 ASPIMATT) is gratefully acknowledged.

*adler@cpfs.mpg.de
†felser@cpfs.mpg.de

[1] T. Graf, S. Parkin, and C. Felser, Prog. Solid State Chem. **39**, 1 (2011).
[2] S. Trudel, O. Gaier, J. Hamrle, and B. Hillebrands, J. Phys. D: Appl. Phys. **43**, 193001 (2010).
[3] J. Kübler, A. R. Williams, and C. B. Sommers, Phys. Rev. B **28**, 1745 (1983).
[4] E. Liu, W. Wang, L. Feng, W. Zhu, G. Li, J. Chen, H. Zhang, G. Wu, C. Jiang, H. Xu, and F. de Boer, Nat. Commun. **3**, 873 (2012).
[5] A. de Campos, D. L. Rocco, A. M. G. Carvalho, L. Caron, A. A. Coelho, S. Gama, L. M. da Silva, F. C. G. Gandra, A. O. dos Santos, L. P. Cardoso, P. J. von Ranke, and N. A. de Oliveira, Nat. Mater. **5**, 802 (2006).
[6] Y. Li, C. B. Jiang, T. Liang, Y. Ma, and H. Xu, Scr. Mater. **48**, 1255 (2003).
[7] C. Felser, G. H. Fecher, and B. Balke, Angew. Chem. **46**, 668 (2007).
[8] J. Winterlik, G. H. Fecher, B. Balke, T. Graf, V. Alijani, V. Ksenofontov, C. A. Jenkins, O. Meshcheriakova, C. Felser, G. Liu, S. Ueda, K. Kobayashi, T. Nakamura, and M. Wojcik, Phys. Rev. B **83**, 174448 (2011).
[9] M. Meinert, J. M. Schmalhorst, G. Reiss, and E. Arenholz, J. Phys. D: Appl. Phys. **44**, 215003 (2011).
[10] S. Wurmehl, G. H. Fecher, H. C. Kandpal, V. Ksenofontov, and C. Felser, Appl. Phys. Lett. **88**, 032503 (2006).
[11] J. Winterlik, B. Balke, G. H. Fecher, C. Felser, M. C. M. Alves, F. Bernardi, and J. Morais, Phys. Rev. B **77**, 054406 (2008).
[12] H. Sukegawa, Z. Wen, K. Kondou, S. Kasai, S. Mitani, and K. Inomata, Appl. Phys. Lett. **100**, 182403 (2012).
[13] M. Gillessen and R. Dronskowski, J. Comput. Chem. **30**, 1290 (2009).
[14] M. Gillessen and R. Dronskowski, J. Comput. Chem. **31**, 612 (2010).
[15] Z. Ren, S. T. Li, and H. Z. Lu, Physica B **405**, 2840 (2010).
[16] J. H. Westbrook and R. L. Fleischer, *Basic Mechanical Properties and Lattice Defects of Intermetallic Compounds* (John Wiley and Sons, Chichester, UK, 2000), Vol. 2, p. 211.
[17] S. Ouardi, G. H. Fecher, B. Balke, A. Beleanu, X. Kozina, G. Stryganyuk, C. Felser, W. Klöss, H. Schrader, F. Bernardi, J. Morais, E. Ikenaga, Y. Yamashita, S. Ueda, and K. Kobayashi, Phys. Rev. B **84**, 155122 (2011).
[18] M. Meinert, J.-M. Schmalhorst, C. Klewe, G. Reiss, E. Arenholz, T. Böhnert, and K. Nielsch, Phys. Rev. B **84**, 132405 (2011).
[19] P. Klaer, C. A. Jenkins, V. Alijani, J. Winterlik, B. Balke, C. Felser, and H. J. Elmers, Appl. Phys. Lett. **98**, 212510 (2011).
[20] P. Soven, Phys. Rev. **156**, 809 (1967).
[21] W. H. Butler, Phys. Rev. B **31**, 3260 (1985).
[22] L. Chapon and J. Rodriguez-Carvajal, FullProf, version 2.0 (2008).
[23] P. Gütlich, E. Bill, and A. X. Trautwein, *Mössbauer Spectroscopy and Transition Metal Chemistry* (Springer-Verlag, Berlin, Heidelberg, 2011), p. 569.
[24] K. Lagarec and D. G. Rancourt, Recoil, version 1.0 (1998).

[25]M. Ellner, K. Kolatschek, and B. Predel, J. Less-Common Met. **170**, 171 (1991).
[26]P. J. Schurer, N. J. G. Hall, and A. H. Morrish, Phys. Rev. B **18**, 4860 (1978).
[27]V. Jung, B. Balke, G. H. Fecher, and C. Felser, Appl. Phys. Lett. **93**, 042507 (2008).
[28]V. Jung, G. H. Fecher, B. Balke, V. Ksenofontov, and C. Felser, J. Phys. D: Appl. Phys. **42**, 084007 (2009).
[29]V. Ksenofontov, M. Wojcik, S. Wurmehl, H. Schneider, B. Balke, G. Jakob, and C. Felser, J. Appl. Phys. **107**, 09B106 (2010).
[30]O. Massenet, H. Daver, V. D. Nguyen, and J. P. Rebouillat, J. Phys. F: Met. Phys. **9**, 1687 (1979).
[31]U. Eberz, W. Seelentag, and H. U. Schuster, Z. Naturforsch. B **35**, 1341 (1980).
[32]H. Ebert, D. Ködderitzsch, and J. Minár, Rep. Prog. Phys. **74**, 096501 (2011).
[33]S. H. Vosko, L. Wilk, and M. Nusair, Can. J. Phys. **58**, 1200 (1980).